Small RNA-Mediated *De Novo* Silencing of *Ac/Ds* Transposons Is Initiated by Alternative Transposition in Maize

Dafang Wang,*,[1] Jianbo Zhang,[†] Tao Zuo,[†] Meixia Zhao,[‡] Damon Lisch,[§] and Thomas Peterson[†,,1]**

*Division of Math and Sciences, Delta State University, Cleveland, Mississippi 38733-0001, [†]Department of Genetics, Development and Cell Biology, and **Department of Agronomy, Iowa State University, Ames, Iowa 50011-3260, [‡]Department of Biology, Miami University, Oxford, Ohio 45056, and [§]Department of Botany and Plant Pathology, Purdue University, West Lafayette, Indiana 47907

ORCID IDs: 0000-0001-8508-0721 (D.W.); 0000-0003-3004-9182 (J.Z.); 0000-0002-6581-1192 (T.Z.); 0000-0001-8812-8217 (M.Z.); 0000-0002-8693-8651 (D.L.); 0000-0002-9933-7556 (T.P.)

ABSTRACT Although transposable elements (TEs) comprise a major fraction of many higher eukaryotic genomes, most TEs are silenced by host defense mechanisms. The means by which otherwise active TEs are recognized and silenced remains poorly understood. Here we analyzed two independent cases of spontaneous silencing of the active maize *Ac/Ds* transposon system. This silencing is initiated by alternative transposition, a type of aberrant transposition event that engages the termini of two nearby separate TEs. Alternative transposition during DNA replication can generate Composite Insertions that contain inverted duplications of the transposon sequences. We show that the inverted duplications of two Composite Insertions are transcribed to produce double-stranded RNAs that trigger the production of two distinct classes of small interfering RNAs: a 24-nt class complementary to the TE terminal inverted repeats and noncoding subterminal regions, and a 21- to 22-nt class corresponding to the TE transcribed regions. Plants containing these small interfering RNA-generating Composite Insertions exhibit decreased levels of *Ac* transcript and heritable repression of *Ac/Ds* transposition. Further, we demonstrate that Composite Insertions can heritably silence otherwise active elements in *trans*. This study documents the first case of transposon silencing induced by alternative transposition and may represent a general initiating mechanism for silencing of DNA transposons.

KEYWORDS *Ac/Ds*; transposon; alternative transposition; inverted duplication; small RNA; transposon silencing

Introduction

Transposable elements (TEs) are often silenced by their hosts, but how TEs are initially recognized for silencing remains unclear. Here we describe two independent loci that induce *de novo* heritable silencing of maize *Ac/Ds* transposons. Plants containing these loci produce double-stranded RNA and *Ac*-homologous small interfering RNAs, and exhibit decreased levels of *Ac* transcript and heritable repression of *Ac/Ds* transposition. We show that these loci comprise inverted duplications of TE sequences generated by alternative transposition coupled with DNA rereplication. This study documents the first case of transposon silencing induced by alternative transposition and may represent a general initiating mechanism for TE silencing.

Transposable elements (TEs) comprise a large proportion of eukaryotic genomes, including those of important crop plants such as rice (>35%, International Rice Genome Sequencing Project, Matsumoto *et al.* 2005), sorghum (62%) (Paterson *et al.* 2009), and maize (85%) (Schnable *et al.* 2009). Over time, multiple sporadic TE proliferations altered the number and distribution of TE sequences, enhancing genome diversity between species and even among varieties of the same species (Tikhonov *et al.* 1999; Sanmiguel and Vitte 2009). These observations indicate that TEs have been, and

doi: https://doi.org/10.1534/genetics.120.303264
Manuscript received December 14, 2019; accepted for publication April 15, 2020; published Early Online April 20, 2020.
Available freely online through the author-supported open access option.
Supplemental material available at figshare: https://doi.org/10.25386/genetics.12150459.
[1]Corresponding authors: Division of Math and Sciences, Delta State University, DSU Box C-4, 1003 W. Sunflower Road, Cleveland, MS 38733-0001. E-mail: dwang@deltastate.edu; and Iowa State University, 2258 Molecular Biology, Iowa State University, Ames, IA 50011-3260. E-mail: thomasp@iastate.edu

continue to be, a major natural force driving genome evolution.

Although uncontrolled TEs can be deleterious to the host (Kidwell 1985), the majority of maize transposons are highly methylated (Regulski *et al.* 2013; West *et al.* 2014) and transcriptionally silenced (Anderson *et al.* 2019), which effectively preserves genome integrity. Small RNA-mediated silencing is an efficient means to initiate and maintain repression of both class 1 (RNA) and class 2 (DNA) TEs. For example, the DNA polymerase IV–RNA-dependent RNA polymerase 2 (Pol IV-RDR2) pathway generates 24-nt small interfering RNAs (siRNAs) to mediate RNA-directed DNA methylation (RdDM) at the homologous DNA targets. Because it relies on transcripts from methylated templates, the Pol IV-RDR2 pathway likely serves to reinforce or maintain silencing of previously silenced TEs [reviewed by Law and Jacobsen (2010), Haag and Pikaard (2011), Castel and Martienssen (2013), and Matzke and Mosher (2014)]. Although the mechanisms of maintenance of TE silencing have been extensively studied, the mechanisms responsible for *de novo* silencing remain relatively obscure. The first evidence for a locus that can silence an active TE came from analysis of *Mu killer* (*Muk)*, a locus that can heritably silence *MuDR* transposons in *trans* in maize. *Muk* comprises an inverted duplication of the *MuDR* 5′ terminal inverted repeat (TIR) and a portion of the *mudrA* gene, which is required for element excision (Lisch 2002). This long inverted repeat is transcribed into double-stranded RNAs (dsRNAs) which initiate siRNA-mediated silencing of intact *MuDR* elements (Slotkin *et al.* 2003, 2005; Li *et al.* 2010). Recent studies of *de novo* silencing of active LTR retroelements in *Arabidopsis* demonstrated the involvement of RdDM (Marí-Ordóñez *et al.* 2013; McCue *et al.* 2014; Duan *et al.* 2015; Panda *et al.* 2016). Active TEs are transcribed by Pol II, followed by second-strand synthesis by RDR6. The resulting dsRNA is then processed into 21- to 22-nt siRNAs (Nuthikattu *et al.* 2013); these 21- to 22-nt siRNAs can then induce post-transcriptional silencing as well as transcriptional gene silencing, which is associated with DNA methylation (Pontier *et al.* 2012; McCue *et al.* 2014; Matzke and Mosher 2014). Once RdDM is initiated, silencing can then be maintained via the classic RdDM pathway, which involves Pol IV-mediated transcription from previously methylated sequences (Matzke and Mosher 2014).

Maize *Ac/Ds* TEs were the first transposons discovered and characterized (McClintock 1948, 1949, 1950, 1951). As members of the class 2 *hAT* transposon superfamily, *Ac/Ds* elements are less numerous than class 1 retroelements, which are often highly amplified (Sanmiguel and Vitte 2009). However, *Ac/Ds* elements can strongly affect gene expression because of their preferential insertions into genes (Vollbrecht *et al.* 2010) and the induction of genome rearrangements via alternative transpositions (Zhang and Peterson 1999). Unlike standard transposition reactions, which act on the 5′ and 3′ termini of a single element, alternative transposition acts on the termini of two separate, usually nearby elements (Gray 2000). During alternative transposition, the termini of two nearby, separate TEs can interact with the transposase and insert into linked or unlinked sites, resulting in various chromosomal rearrangements, including duplications, deletions, inversions, and translocations (Zhang and Peterson 2004; Huang and Dooner 2008; Zhang *et al.* 2009; Wang *et al.* 2015). Moreover, alternative transposition during DNA replication can generate novel structures termed Composite Insertions, which are composed of transposon termini surrounding host genome sequences that were copied from the transposon donor site. Because of their complex and heterogeneous structures, Composite Insertions represent an ongoing source of diverse *Ac* sequence configurations in the genome (Zhang *et al.* 2014)

In a previous study of *Ac/Ds* alternative transposition, Zhang and Peterson (1999) identified an allele termed *p1-ww-id1* that induced significant repression of *Ac/Ds* transposition. Because this stock contains only one copy of *Ac*, the observed *Ac/Ds* repression could not be explained by the classic *Ac* negative dosage effect, in which increased *Ac* copy number results in reduced frequency and developmental delay of *Ac/Ds* transposition (McClintock 1949; Brink Nilan 1952). Subsequently, we isolated a second allele, *p1-ww-id4*, that was independently derived by alternative transposition and that exhibits a similar repression of *Ac/Ds* transposition.

Here, we show that both of these alleles (1) cause *de novo* and heritable repression of *Ac/Ds* transposition and *Ac* mRNA accumulation; (2) contain Composite Insertions with inverted duplications of *Ac* sequence; (3) produce *Ac*-homologous dsRNA transcripts driven by either a flanking host gene promoter or the *Ac* promoter; and (4) accumulate 21-, 22-, and 24-nt siRNAs corresponding to the region of dsRNAs transcribed from each Composite Insertion. The siRNA profile includes two distinct classes: a 24-nt class corresponding to the TIR and subterminal region of *Ac/Ds*, and a 21- to 22-nt class homologous to portions of the transcribed region of *Ac*. These data provide the first evidence for heritable siRNA-mediated silencing of *Ac/Ds* activity. Our results support and extend a previous model of alternative transposition-induced DNA rereplication to generate Composite Insertions (Zhang *et al.* 2014), and also show that the resulting Composite Insertions can trigger heritable silencing of otherwise active elements in *trans*. This study is the first demonstration of *de novo* TE silencing induced by alternative transposition, which may represent a general mechanism of self-repression of class 2 transposons.

Materials and Methods

Maize stocks and screen

The maize *p1* gene regulates pigmentation in floral organs, and *p1* alleles are identified by a two-letter suffix indicating their expression in kernel pericarp (the maternal tissue surrounding the seed) and cob glumes (*e.g.*, "w" for white, "r" for red, and "v" for variegated). The progenitor *p1-vv-9D9A* allele (Zhang and Peterson 1999) contains an active *Ac* element and a *fractured Ac* element (*fAc*; a terminally deleted *Ac* element) inserted into *p1* intron 2. The *p1-vv-9D9A* allele

was introgressed into maize inbred B73, which has a *p1-wr* genotype. To screen for variants in *Ac* activity derived from *p1-vv-9D9A*, silks of plants of genotype *p1-vv-9D9A/p1-wr* were crossed by pollen from an *Ac* tester line of genotype *p1-ww*; *rm-3*::*Ds*. This tester is recessive for a null allele of *p1* and is also homozygous for an *Ds* insertion allele of *r1*, which exhibits excisions in the aleurone of *Ds* in the presence of *Ac* transposase, resulting in colored sectors (Kermicle 1980). The mature ears were screened for multikernel sectors or individual kernels with developmentally delayed (small) purple spots on kernel aleurone due to repressed *Ac* activity. These candidate kernels were then planted and backcrossed to B73 for more than six generations to generate the material for study. After introgression, the final genotype of plants carrying these candidates is *p1-ww-id/p1-wr*; *r1/r1* in B73 background.

Genomic PCR and DNA gel blot hybridizations

Total DNA was prepared from seedling shoots by using a modified cetyltrimethylammonium bromide extraction protocol (Allen *et al.* 2006). HotMaster Taq polymerase (5PRIME) was used in the PCR reactions. PCR reactions were heated at 94° for 2 min; followed by 35 cycles of 94° for 20 sec, 60–68° annealing (depending on primers) for 30 sec, and 65° for 1 min/1 kb expected product length; followed by a final cycle at 65° for 8 min. The sequences of oligonucleotide primers are listed in Supplemental Material, Table S1. For Southern blots, total DNA extracted from seedling shoots was digested with restriction enzymes from Promega and electrophoresed through 0.8% agarose gels. Blotting and hybridization were performed according to standard protocols (Sambrook *et al.* 1989); blots were washed in stringent conditions (0.5% SDS, 0.5×SSC at 60°).

Plant growth and tissue collection

Seeds were germinated in SB300 Universal Mix soil mix, and grown in a PGW-40 growth chamber (Percival Scientific, Perry, IA) at 25° for 15 hr in the light and 20° for 9 hr in the dark. Both the above-ground tissues (shoot) and below-ground tissues (root) were harvested from seedlings 14 days after sowing. Nine random plants were pooled for each genotype and tissue type.

RNA isolation and complementary DNA preparation

Total RNA was extracted from seedling shoots and roots by two methods: (1) using the RNeasy Plant mini kit (QIAGEN, Valencia, CA) for small-scale RNA isolation, and (2) using the PureLink Plant RNA Reagent (Life Technologies) for large-scale RNA isolation. The RNA extracted by both methods was then treated with DNase I (New England Biolabs) to remove residual genomic DNA. The RNA extracted by RNeasy Plant mini kit was then converted to complementary DNA (cDNA) by Omniscript RT kit (QIAGEN) primed with oligo-dT and was used as template in the RT-PCR and quantitative RT-PCR experiment. The RNA used in experiments involving small RNA-sequencing and detection of dsRNAs was extracted using the PureLink Plant RNA Reagent.

Quantitative RT- PCR

Quantitative RT-PCR was performed using the Stratagene Mx4000 multiplex quantitative PCR system. Total RNA and cDNA were prepared as described above. PCR was catalyzed by SsoFast EvaGreen Supermixes (Bio-Rad, Hercules, CA) with two technical repeats and three biological repeats. *Ac* transcript levels measured by primers ac10 and ac11 were normalized by comparison to levels of *ubiquitin* transcript measured by primers Ubi-f and Ubi-r in the same sample as an internal control. The relative expression level of *Ac* in each sample was then calculated by comparison to levels of *Ac* transcript in *p1-vv-9D9A*, which contains a single active *Ac* element. Standard deviations were calculated among replications. Student's *t*-test was then performed to evaluate the differences among samples at significance level of 0.05.

Detection of dsRNAs

Total RNA, prepared as described above, was treated with RNases A/T_1 (Thermo Fisher Scientific) with concentrations of 0, 1.5, and 15 units at 37° for 15 min. The treated RNA was precipitated and reverse transcribed into cDNA by SuperScript III Reverse Transcriptase (Life Technologies) primed with random primers (Thermo Fisher Scientific) as the template for PCR. A seminested PCR was used to amplify regions inside the expected dsRNA (primers ac12 + ac6 followed by ac4 + ac6) to detect dsRNA. Genomic DNA contamination was not detected by using primer ac13 + ac14.

Small RNA high-throughput sequencing and data analysis

Total RNA was extracted as described above and previously (Zuo *et al.* 2016); library preparation and sequencing on Illumina platform HiSeq 2000 were performed by Beijing Genomics Institute. Adapter sequences, contamination, and low-quality reads were filtered from raw data. The small RNA sequences were mapped to *Ac* full-length DNA sequence (4565 bp) by Bowtie (Langmead *et al.* 2009). Only perfectly matched short reads were included in the analysis. The mapped reads from each library were normalized to read counts per million reads.

Data availability

The small RNA high-throughput sequencing data analyzed here is deposited in the NCBI under accession number SRP062285. Maize stocks are available upon request. All data necessary for confirming the conclusions of the article were presented within the article, figures, and tables. Supplemental material available at figshare: https://doi.org/10.25386/genetics.12150459.

Results

The model of sister chromatid transposition-induced DNA rereplication

We previously reported that tandem direct duplications and associated Composite Insertions can be produced by reversed

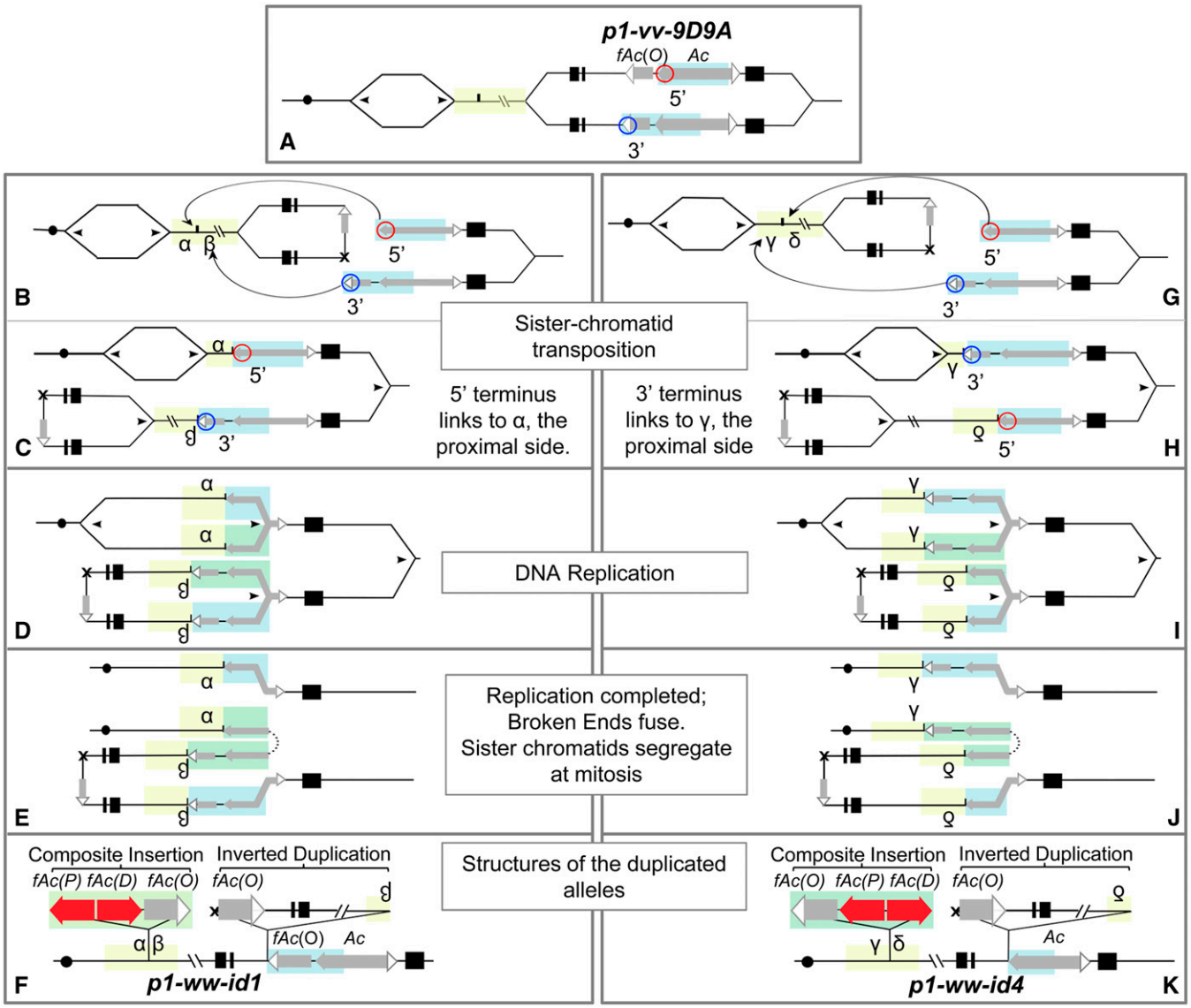

Figure 1 Model of sister chromatid transposition-induced DNA rereplication. (A) Maize chromosome *1* and progenitor allele *p1-vv-9D9A* with DNA replication bubbles. Solid circle indicates centromere. The *p1* gene contains 3 exons (black boxes) with *Ac* and *fAc* elements located in intron 2 (gray boxes with solid/open arrowheads indicate the 5′ and 3′ *Ac/fAc* termini, respectively). The 5′ and 3′ *Ac/fAc* termini involved in sister chromatid transposition are circled in red and blue, respectively. The unreplicated regions are highlighted in yellow, and the replicated regions to be rereplicated are highlighted in blue. (B and C) Sister chromatid transposition, *p1-ww-id1* orientation. (B) Excision of the *Ac* 5′ and *fAc* 3′ termini results in excision footprint (marked by X) and fusion of the two sister chromatids. Curved arrows indicate insertion of the excised transposon ends into the target site (short vertical line). (C) The 5′ terminus of *Ac* is ligated to the centromere-proximal side (marked α) and the 3′ terminus of *fAc* is ligated to the distal side (marked β). This joins the unreplicated sequences at the insertion site to the previously replicated *Ac/fAc* sequences. The replication fork containing the sister chromatid fusion is flipped. (D) DNA replication. As DNA replication continues, *Ac/fAc* sequences are rereplicated (highlighted in green). (E) Completion of DNA replication. Rereplication of *Ac/fAc* sequences aborts, releasing two broken ends that fuse (dotted line). This produces a Composite Insertion between α and β. During mitosis, sister chromatids separate. One sister chromatid (top) has a deletion, and the other sister chromatid (bottom) carries a corresponding inverted duplication and a Composite Insertion between α and β. (F) Maize chromosome *1* with the *p1-ww-id1* allele. The Composite Insertion in the α/β site contains two new *fAc* elements (solid red arrows) containing *Ac* 5′ sequences in inverted orientation: *fAc(P)* (proximal) and *fAc(D)* (distal). *P1-ww-id1* also contains an inverted duplication of the segment from *fAc(O)* (original) to site β. (G and H) Sister chromatid transposition, *p1-ww-id4* orientation. (G) Same as B, except the 3′ terminus of *fAc* will ligate to the centromere-proximal side (marked γ) and the 5′ terminus of *Ac* will ligate with the distal side (labeled as δ) of the insertion site. (H–J) Same as C–E. (K) Maize chromosome *1* containing the *p1-ww-id4* allele. For animation of alternative transposition mechanism, see Supplementary Materials Video 1.

end transposition, a type of alternative transposition, followed by DNA rereplication and repair (Zhang and Peterson 2004; Zhang *et al.* 2014). The Composite Insertions are bordered by partial or full copies of the *Ac* transposon and may also include sequences flanking the original *Ac* donor site. Extending the principle of alternative transposition-induced DNA rereplication, we hypothesized that sister chromatid transposition during DNA replication can produce inverted

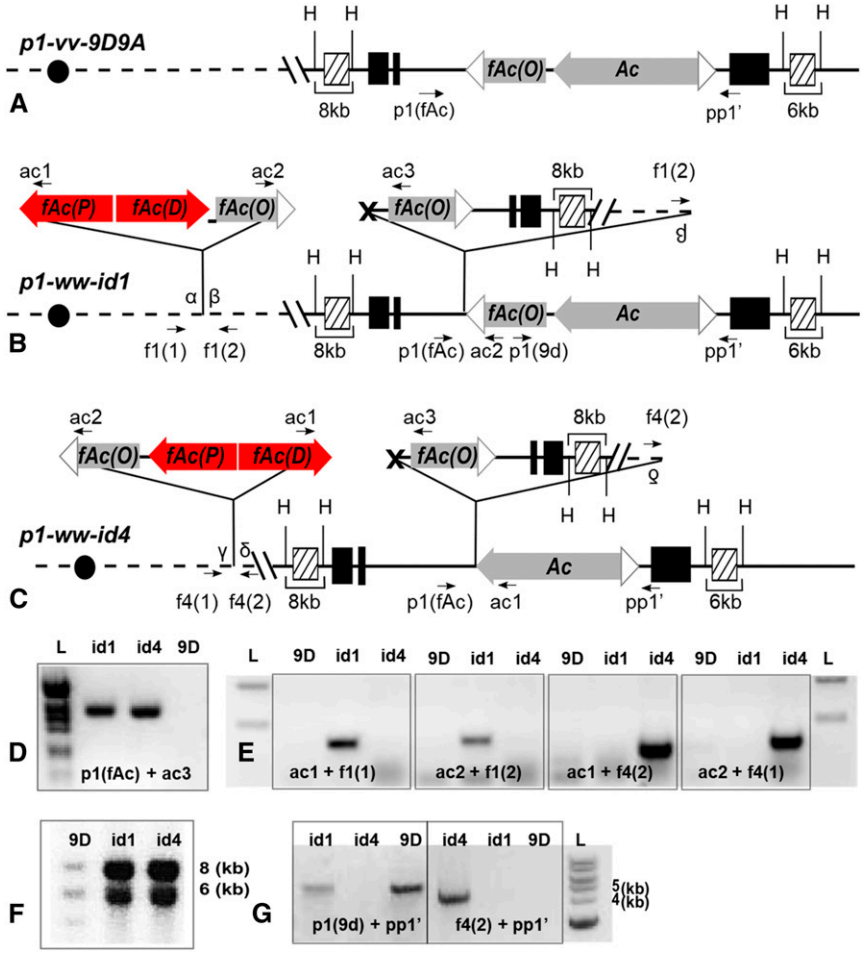

Figure 2 *p1-ww-id1* and *p1-ww-id4* contain Composite Insertions and inverted duplications. (A–C) Structure of the progenitor allele *p1-vv-9D9A* (A), and expected structures of *p1-ww-id1* (B) and *p1-ww-id4* (C) based on the model of sister chromatid transposition-induced DNA rereplication. PCR primers are labeled as arrows, and sequences homologous to hybridization probe *15* are labeled as hatched boxes. H stands for HindIII restriction site. Other symbols are as in Figure 1. (D) Gel analysis of PCR to amplify the sister chromatid transposition footprints in *p1-ww-id1* and *p1-ww-id4*. Bands were excised from the gel and sequenced (File S1). (E) Gel analysis of PCR to amplify the sequences flanking Composite Insertions. Bands were excised from the gel and sequenced to identify the target site duplications flanking each Composite Insertion (File S2). (F) Genomic Southern blot produced by digestion with HindIII and hybridization with probe *15*. (G) Gel analysis of PCRs to determine the orientation of sister chromatid transposition (see text for details).

duplications and Composite Insertions (Figure 1 and Supplemental Material Video 1). In sister chromatid transposition, the *Ac* transposase acts on a pair of directly oriented *Ac* termini that are present in the progenitor allele *p1-vv-9D9A* (Figure 1A). This allele contains a complete *Ac* element inserted 112 bp from a second element termed *fAc*, which contains only the 3′ half of *Ac*. The *Ac* element is known to preferentially transpose during or shortly after S phase (Greenblatt and Brink 1962; Chen *et al.* 1987), possibly because the *Ac* transposase preferentially interacts with hemimethylated *Ac* TIRs (Ros and Kunze 2001). Following replication, the *Ac* 5′ and *fAc* 3′ termini located on sister chromatids have strand-specific hemimethylation patterns that are competent for transposition. Excision of the 5′ and 3′ termini followed by religation of the host sequences flanking these termini is expected to produce a sister chromatid fusion with a small sequence footprint at the excision site (Weil and Wessler 1993) (Figure 1B). The excised termini may then reinsert at many possible genomic sites; for example, they can reinsert at a proximal site to generate reciprocal duplication/deletion chromatids (Figure 1C) (Zhang and Peterson 1999). Insertion of the *Ac* termini into the target site commonly produces 8-bp target site duplications flanking the insertion site, a diagnostic feature of *Ac* transposition (Döring and Starlinger 1984; Peacock *et al.* 1984; Pohlman *et al.* 1984). When sister chromatid transposition from a replicated donor site inserts into an unreplicated target site, previously replicated sequences are joined to unreplicated DNA. As DNA synthesis continues, replication forks progress into the newly inserted *Ac* termini, rereplicating the *Ac/fAc* sequences. Replication may continue into the flanking DNA and extend for 10 kb or more (Zhang *et al.* 2014) (Figure 1D). Ultimately, the DNA rereplication forks spontaneously abort, producing two broken ends that fuse together (McClintock 1951). In some cases, fusion of the two broken ends can generate two *fAc* elements in an inverted orientation, as shown in Figure 1E. In the ensuing mitosis, the two sister chromatids segregate into two daughter cells: one contains a deletion (*p1-ww-def*) and the other contains an inverted duplication (*p1-ww-id*) with a Composite Insertion. In the Composite Insertion, the two new *fAcs* are both derived from *Ac* 5′ termini and are in an inverted orientation relative to each other. We term the proximal one *fAc(P)*, and the distal one *fAc(D)*, to distinguish them from the original *fAc(O)* in the progenitor *p1-vv-9D9A* allele (Figure 1F). Two possible orientations of insertion are predicted by the model: (1) the 5′ terminus of *Ac* ligates to the proximal side of the insertion target (Figure 1, B–F), and (2) the 3′ terminus of *Ac* ligates to

the proximal side of the insertion target (Figure 1, G–K). These two orientations are found in the *p1-ww-id1* and *p1-ww-id4* alleles, respectively.

Alleles p1-ww-id1 and p1-ww-id4 contain structural hallmarks expected from the model of sister chromatid transposition-induced DNA rereplication

Figure 2 summarizes the structural features of the *p1-vv-9D9A*, *p1-ww-id1*, and *p1-ww-id4* alleles (Figure 2, A–C.) As predicted by the sister chromatid transposition model, both *p1-ww-id1* and *p1-ww-id4* contain Composite Insertions and inverted duplications as compared to the progenitor *p1-vv-9D9A*. To further test the model, we examined the sequences at the junctions of the inverted duplications. As previously reported (Zhang and Peterson 1999), *p1-ww-id1* contains a typical *Ac* excision footprint at the junction of the inverted duplication segments. For *p1-ww-id4*, we PCR-amplified and sequenced the excision site [using primers ac3 + p1(fAc) in Figure 2C; results shown in Figure 2D]. Similar to the footprint of *p1-ww-id1* (Zhang and Peterson 1999), *p1-ww-id4* shows changes at the first nucleotides flanking the *Ac/fAc* excision sites, as is typical for sites of *Ac* excision (File S1).

We then isolated the sequences flanking the Composite Insertions in each allele by inverse PCR, and confirmed the insertion junctions by direct PCR using primer pairs f1(1) + ac1 for *p1-ww-id1*, and f4(2) + ac1 for *p1-ww-id4* (Figure 2E). The sequences flanking the Composite Insertions contain perfect 8-bp target site duplications ("GCCTCGCT" in *p1-ww-id1* and "GCCCGGAT" in *p1-ww-id4*; File S2) characteristic of *Ac* transposition.

The sister chromatid transposition model predicts that the *p1-ww-id1* and *p1-ww-id4* alleles contain inverted duplications extending from the *p1* locus at 48.6 Mb of maize chromosome *1* to the Composite Insertion sites. The sequences flanking the Composite Insertions in *p1-ww-id1* and *p1-ww-id4* are located at positions 51.8 and 48.9 Mb, respectively, on chromosome *1*, maize B73 RefGen_v4 reference genome. These results indicate that the *p1-ww-id1* and *p1-ww-id4* contain inverted duplications of 3.2 and 0.3 Mb, respectively.

The presence of duplicated segments in *p1-ww-id1* and *p1-ww-id4* is tested by Southern blot using HindIII digests and probe fragment *15* (Figure 2F). The fragments of 8 and 6 kb originate from the proximal and distal side of *p1*, respectively. In the progenitor allele *p1-vv-9D9A* (labeled as 9d), the intensities of the 8- and 6-kb bands are approximately equal, consistent with their single-copy status in *p1-vv-9D9A*. In the *p1-ww-id1* and *p1-ww-id4* alleles, the 8-kb band intensity is approximately twice that of the 6-kb band, consistent with a duplication of the 8-kb segment proximal to *p1* in those alleles. Hybridization signals in lane 9d are overall weaker due to the fact that there is less DNA loaded on the gel. This experiment confirms the presence of a duplication extending to the proximal side of *p1* as predicted by the sister chromatid transposition model.

Finally, we tested the orientations of the Composite Insertions in the *p1-ww-id1* and *p1-ww-id4* alleles. These

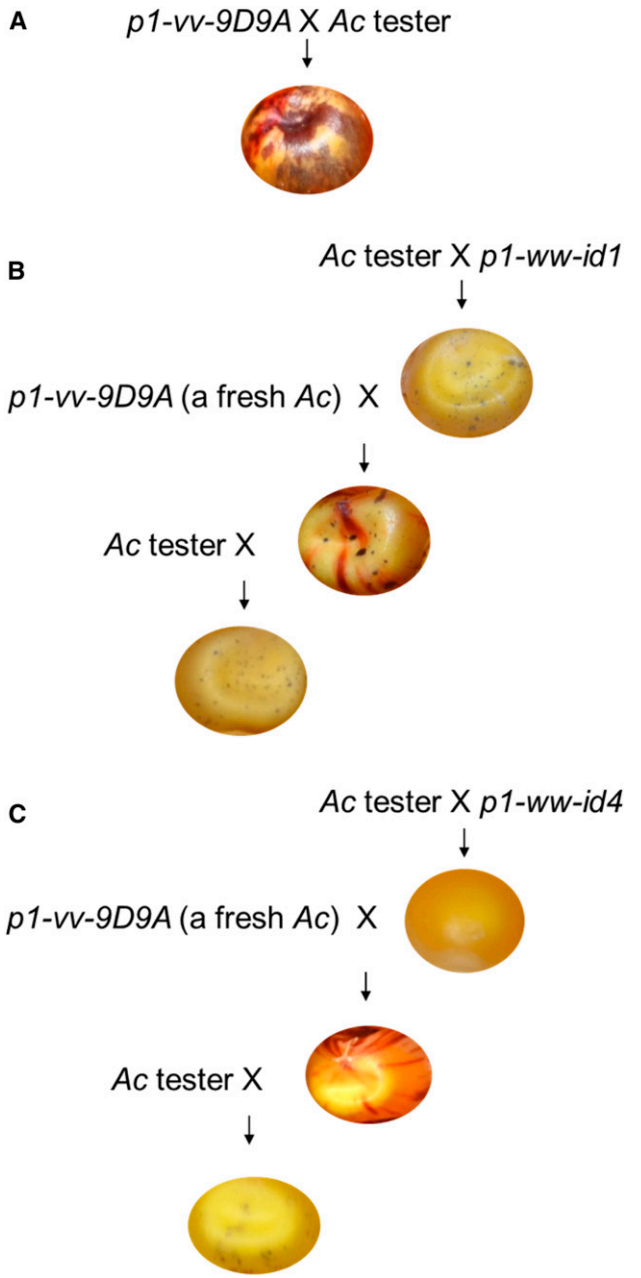

Figure 3 Genetic crosses indicate the *in-trans* and heritable repression of *Ac/Ds* initiated by *p1-ww-id1* and *p1-ww-id4*. (A) Progenitor allele *p1-vv-9D9A* contains a single active *Ac* element, shown by the heavily spotted kernel aleurone from the cross of *p1-vv-9D9A* and *Ac* tester. Cross: *p1-vv-9D9A* x *r1-m3*::*Ds*. (B) *Ac* activity is repressed in *p1-ww-id1*, shown by the fine spots in kernel aleurone in the first cross of *p1-ww-id1* and *Ac* tester (*p1-vv-id1* x *r1-m3*::*Ds*). The second cross (*p1-vv-9D9A x p1-ww-id1*) introduces a fresh active *Ac* in *p1-vv-9D9A*, which is repressed in *trans* by *p1-ww-id1 (*indicated by small aleurone spots). The third cross (*r1-m3*::*Ds x p1-vv-9D9A/p1-ww-id1*) shows that silencing of *Ac* in *p1-vv-9D9A* is heritable, as small spots are maintained even after *p1-vv-9D9A* is segregated from *p1-ww-id1*. (C) Parallel crosses of *p1-ww-id4* as in B. *Ac* activity is repressed in the line of *p1-ww-id4*, shown as absence of kernel aleurone spots in the first cross between *p1-ww-id4* and *Ac* tester. The repression is *trans*-dominant, shown by the absence of spots in kernels produced by cross of active *Ac* from *p1-vv-9D9A* by *p1-ww-id4. Ac* repression is heritable, shown by the fine spotting in kernels from the third cross in which *p1-vv-9D9A* is segregated from *p1-ww-id4*.

orientations depend on whether the excised 5′ *Ac* and 3′ *fAc(O)* are joined to the proximal or distal sides of the Composite Insertion site (Figure 1, B and G), and are correlated with the presence or absence of *fAc(O)* adjacent to *Ac* in the original *p1* donor site (Figure 1, F and K). Therefore, we used PCR primers p1(9d) + pp1' to amplify from *fAc(O)* across *Ac* and into the flanking *p1* gene sequence, producing a 6.6-kb product; this 6.6-kb product was observed in *p1-ww-id1* and the control *p1-vv-9D9A*, but not *p1-ww-id4* (Figure 2G). This result indicates that in *p1-ww-id1*, the 3′ terminus of *fAc(O)* is ligated to the centromere-distal side of the target site (β in Figure 1B). Conversely, primers f4(2) and pp1' produce a 4.5-kb band from *p1-ww-id4*, but not *p1-ww-id1* and *p1-vv-9D9A* (Figure 2G). This 4.5-kb band reflects the absence of *fAc(O)* adjacent to *Ac* in the *p1-ww-id4* allele, indicating that in *p1-ww-id4*, the 5′ terminus of *Ac* is ligated to the centromere-distal side of target site (δ in Figure 1G). In summary, these results show that the *p1-ww-id1* and *p1-ww-id4* alleles contain transposon donor excision footprints, Composite Insertions in two possible orientations flanked by target site duplications, and proximal duplications, all as predicted by sister chromatid transposition with insertion into unreplicated target sites.

p1-ww-id1 and p1-ww-id4 alleles induce de novo and heritable silencing of Ac

The maize *p1* gene is required for kernel pericarp (seed coat) pigmentation (Zhang and Peterson 1999). The *p1-vv-9D9A* allele contains an *Ac* element in *p1* intron 2 (Figure 2A), which blocks *p1* expression and results in colorless pericarp. Somatic excision of *Ac* can restore *p1* function and thus produce red clonal sectors on the kernel pericarp (a variegated pericarp phenotype). The *p1-vv-9D9A* allele produces frequent kernel pericarp sectors, indicating that the *Ac* in *p1-vv-9D9A* is fully active. This is confirmed by crosses of *p1-vv-9D9A* to an *Ac* tester line of genotype *r1-m3*::*Ds* (Figure 3A). The *Ac* tester line contains a nonautonomous *Ds* element inserted in *r1* (*red1*), a gene required for anthocyanin biosynthesis in kernel aleurone. Without an active *Ac*, the *Ds* insertion blocks *r1* function, resulting in colorless aleurone; however, with an active *Ac*, *Ds* can be transposed from *r1*, producing purple aleurone sectors (Kermicle 1980; Lechelt *et al.* 1989). The activity of *Ac* can thus be assessed by the size and frequency of purple spots on the kernel: large spots from early *Ds* excision events indicate a fully active *Ac*, while small spots from delayed *Ds* excisions indicate repressed *Ac* activity. As shown in Figure 3A, crosses of *p1-vv-9D9A* to the *Ac* tester line produce kernels with a coarsely spotted pattern typical of active *Ac*. In contrast, crosses of *p1-ww-id1* with *Ac* testers produce kernels with fine spots (Figure 3B, top kernel), while *p1-ww-id4* gives no spots in test crosses (Figure 3C, top kernel). These results suggest that the *Ac* elements in *p1-ww-id1* and *p1-ww-id4* are repressed. Moreover, *p1-ww-id1* and *p1-ww-id4* can induce *trans*-dominant repression of a fresh and active *Ac*. This can be seen in the kernels produced by crossing *p1-ww-id* alleles to the *p1-vv-9D9A* allele that

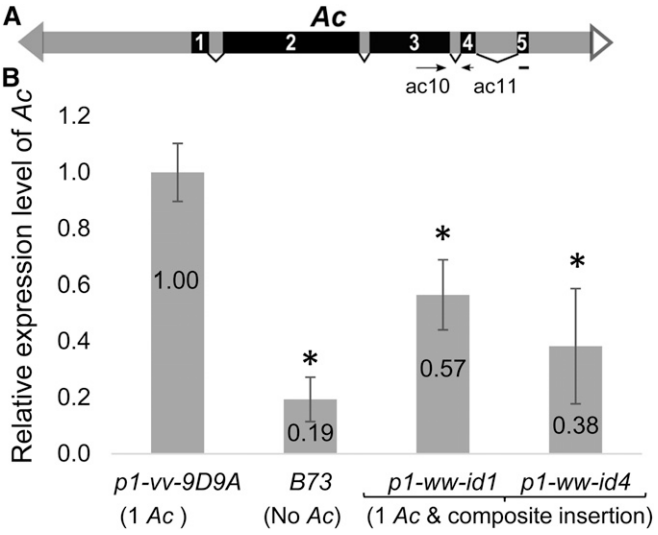

Figure 4 The *Ac* transcript level is decreased in *p1-ww-id* alleles. (A) Schematic structure of the full-length *Ac* transposable element. Solid and open triangles indicate *Ac* 5′ and 3′ termini, respectively. Black boxes with numbers are *Ac* exons 1–5; boxes with subtending lines indicate introns. Primers used in the quantitative RT PCR (ac10 and ac11) are labeled as arrows; note that primer ac11 spans *Ac* intron 4. (B) Quantitative RT-PCR measurement of *Ac* transcript levels. Bars labeled by * indicate transcript levels that are significantly different from *p1-vv-9D9A* by Student's unpaired *t*-test with $P < 0.05$.

contains a single active *Ac*. Kernels heterozygous for *p1-vv-9D9A/p1-ww-id1* show very few and fine aleurone sectors (Figure 3B, second kernel), while kernels produced by crossing *p1-vv-9D9A* with *p1-ww-id4* had no visible aleurone sectors (Figure 3C, second kernel). Note that these kernels exhibit a normal variegated pericarp phenotype because the kernel pericarp is a maternal tissue and thus is not affected by a repressive *p1-ww-id* allele introduced through the pollen in this cross.

To test whether the repression of *Ac* induced by *p1-ww-id1* and *p1-ww-id4* reflects heritable silencing, we crossed *p1-vv-9D9A/p1-ww-id* plants to the *Ac* tester line; this cross separates the *Ac* element in *p1-vv-9D9A* from each *p1-ww-id* allele. If the repression of *Ac* in *p1-vv9D9A* is relieved following segregation from *p1-ww-id*, then we would expect to see ~50% coarsely spotted kernels (containing *p1-vv-9D9A*) and ~50% weakly or nonspotted kernels (containing *p1-ww-id*). However, if *Ac* is heritably silenced, then most or all progeny kernels would again show few, small *Ds* excision sectors. The results show that all the kernels produced by crossing *p1-vv-9D9A/p1-ww-id1* with the *Ac* tester show few or zero purple sectors (0% heavily spotted seeds; Figure 3B, third kernel). The corresponding ear for this cross is shown in Figure S1, and kernel count data are provided in Table S2, Cross 6. Parallel genetic tests show that *Ac* repression induced by *p1-ww-id4* is also heritable, but is less stable than that induced by *p1-ww-id1*. Among 160 progeny kernels from the cross of *Ac* tester by *p1-vv-9D9A/p1-ww-id4*, 126 are weakly or nonspotted (Figure 3C, third kernel), and 34 kernels are heavily spotted. Assuming the heavily

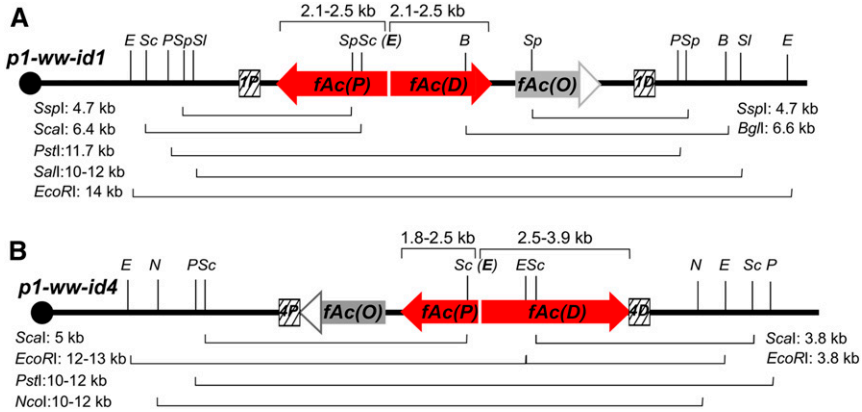

Figure 5 Summary of Southern blot results that elucidate the internal structures of Composite Insertions. Schematic structures of *p1-ww-id1* and *p1-ww-id4* are shown in A and B, respectively, with restriction sites (vertical lines; E: EcoRI; Sc: ScaI; P: PstI; Sp: SspI; Sl: SalI; B: BglI; N: NcoI) and probes (hatched boxes) shown. Bands observed from Southern blot (Figures S3 and S4) are indicated by braces with actual sizes labeled by each restriction enzyme.

spotted kernels are derived from a reactivated *Ac* in the *p1-vv-9D9A* allele, this indicates that *Ac* repression is lifted in 42.5% (34/80) of kernels following segregation from *p1-ww-id4* (Fisher exact test $P < 0.00001$, indicating a significant difference from the *p1-vv-9D9A* ear without the initial silencing; ear for this cross is shown in Figure S2, and kernel count data are provided in Table S2, cross 8). In other words, the silencing of *Ac* induced by *p1-ww-id4* is heritable in only ~57.5% of the progeny kernels that carry *p1-vv-9D9A*.

We also assessed the maintenance of *Ac* silencing in succeeding generations following segregation from the *p1-ww-id1* and *p1-ww-id4* alleles. Plants of genotype *p1-vv-9D9A*/p1-ww* (weakly spotted kernels, where * indicates *Ac* silenced by exposure to *p1-ww-id1* or *p1-ww-id4* in the prior generation) were crossed again to the *Ac* tester stock *r1-m3*::*Ds*. In these crosses, 50% of the kernels receive *p1-ww* (no *Ac*) and are nonspotted, while the remaining 50% of kernels receive *p1-vv-9D9A** and their spotting pattern can reflect the stability of *Ac* silencing. Interestingly, *p1-ww-id1* and *p1-ww-id4* induce different levels of silencing stability. For *p1-vv-9D9A** initiated by *p1-ww-id1* and separated from it for two generations, all the kernels are nonspotted or weakly spotted, indicating near complete maintenance of *Ac* repression (Figure S1; Table S2, cross 7). In contrast, the silencing of *Ac* initiated by *p1-ww-id4* and segregated from it for two generations is not efficiently maintained. Among 144 progeny seeds from the cross of *Ac* tester by *p1-vv-9D9A/p1-ww*, 72 seeds are expected to inherit the *p1-vv-9D9A* allele and thus contain *Ac*. In the progeny kernels we observed 52 heavily spotted seeds, meaning that *Ac* is reactivated in 72.2% (52/72) of the kernels (Fisher exact test *P*-value is 0.0116, indicating a significant difference from the *p1-vv-9D9A* ear without the initial silencing; Figure S2; Table S2, cross 9). Thus, the repression of *Ac* initiated by *p1-ww-id4* is maintained in only ~27.8% of progeny kernels after two generations.

To determine the mechanism of *Ac* repression, we performed quantitative RT-PCR experiment using *Ac*-specific primers. Compared to the progenitor allele *p1-vv-9D9A*, the *p1-ww-id1* and *p1-ww-id4* alleles express significantly decreased levels of *Ac* transcript (Student's *t*-test $P = 0.0015$ and 0.0004, respectively) (Figure 4), suggesting that repression occurred via transcriptional and/or post-transcriptional gene silencing.

Composite Insertions of alleles p1-ww-id1 and p1-ww-id4 contain inverted repeats of fAc fragments

We performed genomic Southern blots to determine the structures of the Composite Insertions in *p1-ww-id1* and *p1-ww-id4*. The results are summarized in Figure 5, and the raw data are shown in Figure S3 and Figure S4. First, the sizes of Composite Insertions are estimated by using restriction enzymes that do not cut within the *Ac* element. For *p1-ww-id1*, digestion with SalI and hybridization with probe *1D* gives a band of 10–12 kb, indicating a Composite Insertions of ~6.2–8.2 kb. Consistent with this, enzyme PstI and probe *1P* give an estimated size of ~6.7 kb. We then determined the internal Composite Insertion structure by digesting with a series of endonucleases with known sites in *Ac*. We observed the expected bands produced by digestion at the SspI and ScaI sites in *fAc(P)*, and the expected bands from digestion at the SspI of *fAc(O)* and BglI sites of *fAc(D)*. These results indicate that the Composite Insertion of *p1-ww-id1* includes the first 1842 bp sequences from the *Ac* 5′ terminus of *fAc(P)* and the first 729 bp sequences from *fAc(D)*. If either *fAc(P)* or *fAc(D)* contained the EcoRI site located near the center of *Ac*, then digestion with EcoRI and hybridization with probe *1P* would yield a band of size 7.6–9.6 kb. No such band is observed, and instead we detect a larger band of ~14 kb. This indicates that both *fAc(P)* and *fAc(D)* were truncated prior to reaching the EcoRI site at position 2486 bp from the *Ac* 5′ end. We conclude that the total size of Composite Insertion in *p1-ww-id1* is <7.1 kb, consistent with the ~6.7 kb size estimated by PstI digestion.

Similar assays were performed on *p1-ww-id4* (Figure 5B and Figure S4). PstI and NcoI digestions both show the total size of the Composite Insertion in *p1-ww-id4* as ~6.4–8.4 kb. The Composite Insertion contains the ScaI site in both *fAc(P)* and *fAc(D)*, indicating that both *fAc* fragments include at least 1842 bp of *Ac* 5′ terminal sequences. Additionally, *fAc(D)* contains the EcoRI site but *fAc(P)* does not, indicating that *fAc(P)* is truncated prior to the EcoRI site at position 2486 bp from *Ac* 5′ terminus. Combining the results from ScaI and EcoRI

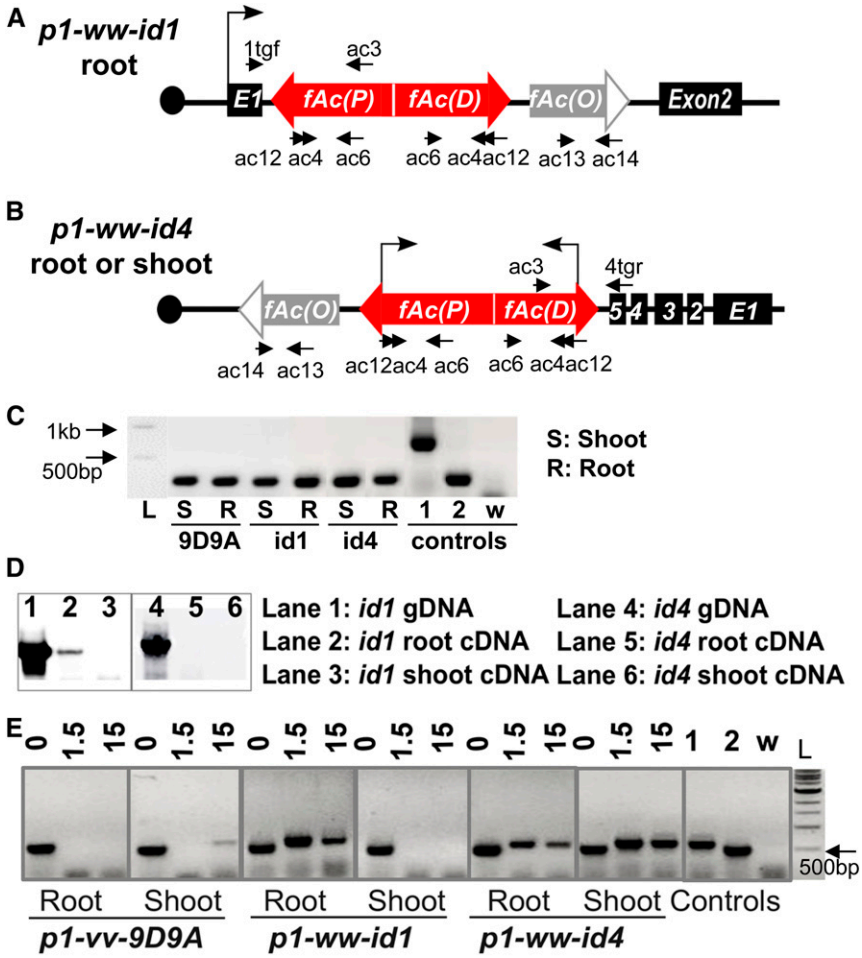

Figure 6 Composite Insertions in *p1-ww-id1* and *p1-ww-id4* produce dsRNA transcripts. (A) Structure of the Composite Insertion in *p1-ww-id1*, located in intron 1 of gene Zm00001d028930. Bent arrow indicates transcription from the host gene promoter to generate read-through transcripts of the Composite Insertion in root tissues, but not shoot. Labeled arrows indicate primers used in RT-PCR. (B) Structure of the Composite Insertion in *p1-ww-id4*, located in intron 5 of Zm00001d028863. The promoter of Zm00001d028863 is not active in either root or shoot tissues. Bent arrows indicate transcription from the native *Ac* promoters. (C) Test of genomic DNA contamination in RNA samples. Primers ac13 + ac14 are located in *fAc(O)* outside the dsRNA region, in *Ac* exons 3 and 5 (Figure 6, A and B). Bands of 744 bp and 272 bp are expected from genomic DNA and spliced cDNA, respectively. Control lanes "1" and "2" are from templates of genomic DNA and root cDNA, respectively, of *p1-ww-id1*; lane "w" is from a water template as a control for PCR contamination. (D) Test for chimeric transcripts by RT-PCR using primers 1tgf + ac3 in *p1-ww-id1* (lanes 1–3), and 4tgr + ac3 in *p1-ww-id4* (lanes 4–6). Chimeric transcript initiating from flanking gene promoter was detected only in *p1-ww-id1* root. No chimeric transcript from flanking gene promoter was detected in *p1-ww-id4*. (E) Detection of dsRNA by RNase protection assay. Total RNA from the indicated tissues and alleles were treated with DNase1 and three quantities of RNase A/T_1 (0, 1.5, and 15 units). Treated RNA samples were then analyzed by a seminested PCR (primers ac12 + ac6; followed by ac4 + ac6). Control lanes "1" and "2" are from templates of genomic DNA and root cDNA, respectively, of *p1-ww-id1*; lane "w" is from a water template as a control for PCR contamination.

digests, the size of *fAc(P)* could be from 1842 to 2486 bp. By subtracting the size of *fAc(P)* (1.8–2.5 kb) from the total size of Composite Insertion of *p1-ww-id4* (6.4–8.4 kb), we infer the size of *fAc(D)* is 2.5–3.9 kb. Extensive attempts were made to PCR amplify and sequence the exact fusion point connecting *fAc(D)* and *fAc(P)* in both Composite Insertions; unfortunately, these attempts failed, most likely due to the long perfectly inverted repeats present in both Composite Insertions, which would give rise to self-annealed hairpins with extensive secondary structures in the template DNA.

The inverted repeats of fAc fragments are transcribed to produce dsRNAs

The inverted *fAc(P)* and *fAc(D)* fragments in both *p1-ww-id1* and *p1-ww-id4* retain the *Ac* promoter. Moreover, consistent with the characteristic preferential insertions of *Ac/Ds* into linked genes (Vollbrecht *et al.* 2010), both Composite Insertions are located in the middle of annotated maize genes: the Composite Insertion in *p1-ww-id1* is located at intron 1 of Zm00001d028930, while the Composite Insertion in *p1-ww-id4* is located at intron 5 of Zm00001d028863 (Figure 6, A and B). The locations of Composite Insertions within genes could allow their expression by read-through transcription from the flanking genes' promoters.

To test for read-through transcription, we performed RT-PCR experiments using total RNA extracted from root and shoot tissues of plants containing *p1-ww-id1* and *p1-ww-id4*. No genomic DNA contamination is detected as illustrated in Figure 6C. For *p1-ww-id1*, chimeric transcripts are detected in root, but not shoot (Figure 6D); this is the same pattern of expression as the flanking host gene Zm00001d028930 (Wang *et al.* 2009) (Figure S5). The chimeric transcript includes sequences from exon 1 and intron 1 of the host gene Zm00001d028930, and sequences from the 5′ terminus of *Ac* (File S3), consistent with the structure expected of read-through transcripts. In contrast, gene Zm00001d028863, the host gene of the Composite Insertion of *p1-ww-id4*, is not expressed in either root or shoot, and we did not detect chimeric *p1-ww-id4* transcripts in those tissues (Figure 6D).

Prompted by the inverted *fAc* repeat structures in both *p1-ww-id1* and *p1-ww-id4* Composite Insertions, we searched for *Ac*-homologous dsRNAs using RNA protection assays. In this experiment, total RNA samples were treated with two concentrations of RNase A/T; linear RNAs can be digested by the RNase, while dsRNAs are resistant. Following RNase treatment,

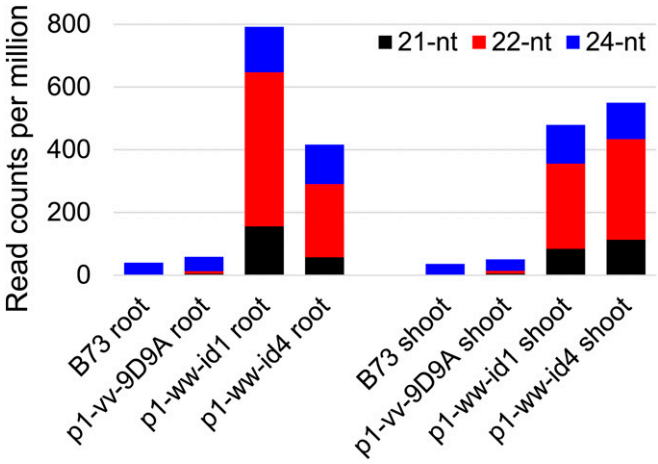

Figure 7 Small RNAs mapped to *Ac*. Compared to inbred B73 and progenitor allele *p1-vv-9D9A*, small RNA levels are increased significantly in both *p1-ww-id1* and *p1-ww-id4*. Colored bars indicate the abundance of 21-, 22-, and 24-nt small RNA classes.

RNAs were reverse transcribed into cDNA, which was used as template for PCR. A seminested PCR was performed to detect sequences protected by dsRNA (primers ac12 + ac6 followed by ac4 + ac6; Figure 6, A and B). We observed bands of the expected size in *p1-ww-id1* root, but not shoot. This pattern matches the expression pattern of the host gene Zm00001d028930 and of the presence of chimeric transcripts. We also detected *Ac*-homologous dsRNAs in both root and shoot of *p1-ww-id4* (Figure 6E), suggesting that *p1-ww-id4* may be transcribed from its own *Ac* promoter. Interestingly, both the chimeric transcript and the dsRNAs seem to retain introns (Figure 6, D and E and File S3), suggesting that the hairpin nature of these transcripts may interfere with normal splicing.

We concluded that the inverted repeats of *fAc* elements in the Composite Insertions of *p1-ww-id1* and *p1-ww-id4* are transcribed into dsRNAs, either by the flanking gene promoter as in *p1-ww-id1*, or by the retained *Ac* promoter as suggested for *p1-ww-id4*. The accumulation of dsRNAs can thus provide a potential template for production of siRNAs that may directly induce *Ac* silencing.

Small RNAs derived from Composite Insertions are detected in both p1-ww-id1 and p1-ww-id4 alleles

The presence of dsRNAs in *p1-ww-id1* and *p1-ww-id4* suggests a possible mechanism of *Ac* silencing by siRNAs. Therefore we performed high-throughput sequencing of small RNAs from root and shoot tissues of *p1-ww-id1* and *p1-ww-id4* plants. Progenitor allele *p1-vv-9D9A* and standard maize inbred B73 were used as controls. As shown in Figure 7, siRNAs of 21, 22, and 24 nt that map to *Ac* are dramatically enriched in both shoot and root from both *p1-ww-id1* and *p1-ww-id4* plants compared to the same tissues in *p1-vv-9D9A* and B73. In *p1-ww-id1* root and shoot, the enriched small RNAs map to a 1- to 2486-nt region from the *Ac* 5′ terminus (Figure 8), consistent with the extent of dsRNA predicted by the Composite Insertion inverted repeat structure. In *p1-ww-id4*, the enriched small RNAs map to the region 1–3400 nt from the *Ac* 5′ terminus, again matching the expected stem-loop structure with the size range of 2486–3900 nt predicted by the Composite Insertion structure. This finding suggests that small RNAs are synthesized from both the double-strand stem and single-strand loop regions of *p1-ww-id4*.

Interestingly, the different size-classes of siRNAs map to distinctly different regions of *Ac*. The 24-nt siRNAs are enriched in the 5′ TIR/sub-TIR regions of *Ac* (Figure S6, B–D); this region includes the native *Ac* promoter and the presence of these 24-nt small RNAs is consistent with a Pol IV/RDR2-based maintenance of heritable silencing (Law and Jacobsen 2010; Pikaard 2013; Matzke and Mosher 2014; Li *et al.* 2015a). In contrast, the 21- to 22-nt siRNAs predominate in the transcribed regions of *Ac* (Figure S6E). This size of siRNAs have been shown to be associated with the Pol II-RDR6 pathway (Pontier *et al.* 2012; Marí-Ordóñez *et al.* 2013; Nuthikattu *et al.* 2013; Matzke and Mosher 2014; McCue *et al.* 2014; West *et al.* 2014; Duan *et al.* 2015; Panda *et al.* 2016) and thus may induce *de novo* silencing of active *Ac* elements. The 21- to 22-nt siRNAs are also mapped to the single-strand loop region in *p1-ww-id4* (Figure 8; the expanded loop region is shown in Figure S7). This is consistent with a transitive process, by which RDR6 converts the single-stranded RNAs in the loop into dsRNAs, followed by the processing of dsRNAs into small RNAs. The ratio of 21- to 22-nt siRNA is increased in the loop region in shoot compared to root tissues (Table S3; chi-squared test gives $P < 0.01$ in shoot and $P = 0.24$ in root), suggesting tissue-specific variation in production or stability of siRNA species. Finally, we noted that 21-nt siRNAs in *p1-ww-id1* are enriched in *Ac* intron sequences, consistent with the observation that both the chimeric *Ac* transcript and dsRNAs retain introns in *p1-ww-id1* (Figure S8).

We observed similar profiles of siRNA in both root and shoot tissues of *p1-ww-id1*, even though no Composite Insertion transcripts or dsRNAs were detected in *p1-ww-id1* shoots. Possibly, this might result from long-range transportation of siRNAs from root (where dsRNAs are produced) to shoot (where dsRNAs are absent), as described previously in *Arabidopsis* (Chitwood and Timmermans 2010; Molnar *et al.* 2010). In any event, the fact that the siRNAs in *p1-ww-id1* and *p1-ww-id4* correspond well to the structure of the two Composite Insertions in each allele strongly suggests that these Composite Insertions are the source of the siRNAs.

Discussion

In this study, we characterized two naturally occurring maize alleles (*p1-ww-id1* and *p1-ww-id4*) derived by alternative transposition of the transposable element *Ac*. Both alleles elicit *trans*-dominant and heritable repression of *Ac*-induced transposition, reduce accumulation of *Ac* mRNA, and contain inverted duplications and novel Composite Insertions derived from sister chromatid transposition-induced DNA rereplication.

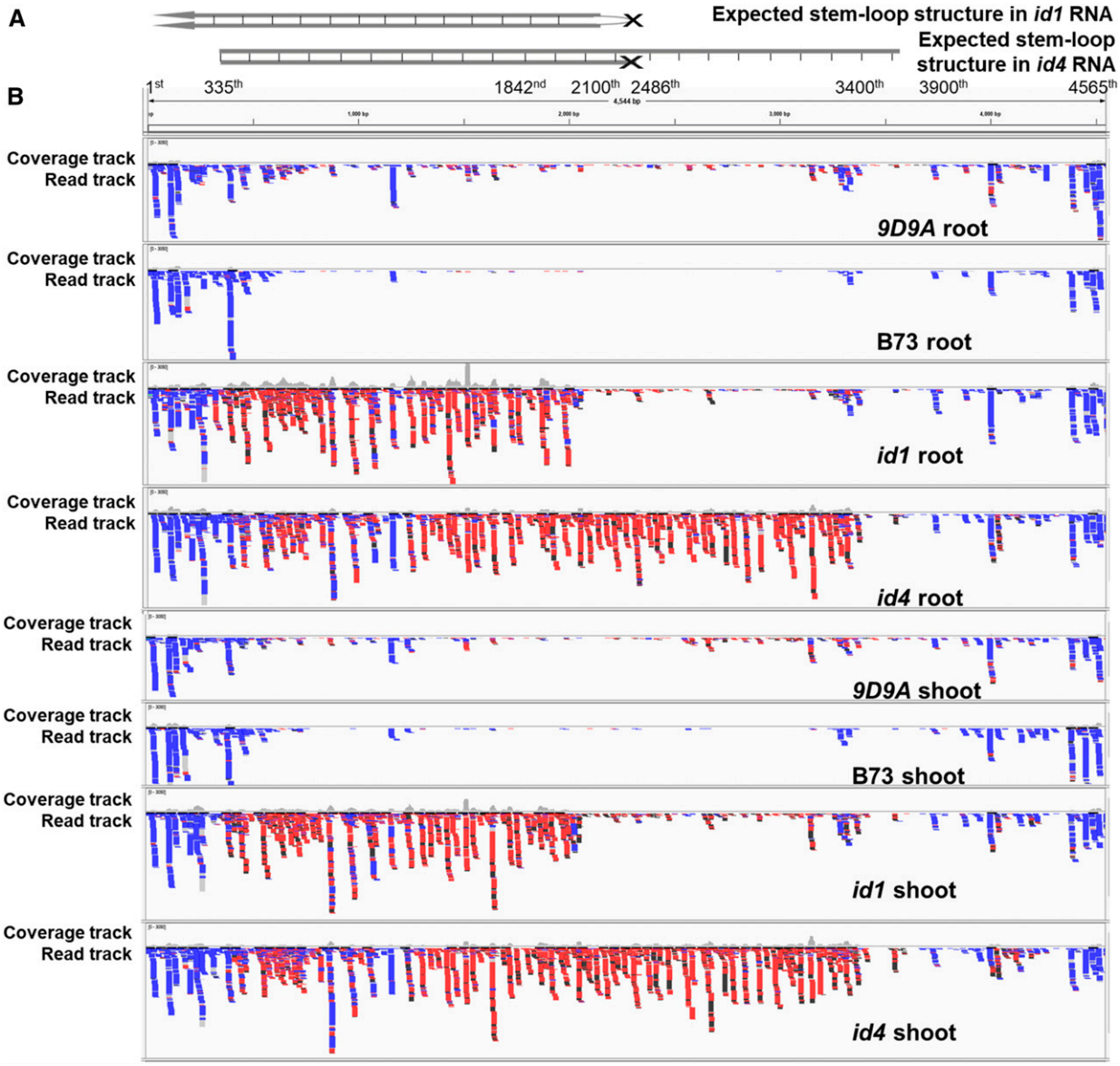

Figure 8 Detection and mapping of small RNAs in *p1-ww-id1* and *p1-ww-id4*. (A) The expected stem-loop structures in *p1-ww-id1* and *p1-ww-id4*. The schematic structures include a ruler with corresponding nucleotide position in *Ac*. The loop of *p1-ww-id4* is open for better presentation of the size. The transcription of Composite Insertion of *p1-ww-id1* is driven by the host promoter, and the two inverted *fAc* fragments in *p1-ww-id1* are relatively symmetrical (2100–2486 nt of each indicated by Southern blot), predicting a hairpin structure in the dsRNA contains first ~ (2100th–2486th) nucleotides of *Ac*. The transcription of Composite Insertion of *p1-ww-id4* is driven by the *Ac* promoter, and thus the transcript starts from 335th nucleotide of *Ac*. The inverted *fAc* fragments in *p1-ww-id4* differ in size, with one *fAc* fragment of 1842–2486 nt and the other *fAc* of 3400–3900 nt indicated by Southern blot. This asymmetrical structure should give rise to a transcript with a stem containing 335th ~ (1842nd–2486th) nucleotides of *Ac* and a loop containing (1843rd–2487th) ~ (3400th–3900th) nucleotides of *Ac* in *p1-ww-id4*. (B) Small RNAs mapped to *Ac* are visualized by the Integrative Genomics Viewer (Robinson *et al.* 2011). The y axis of the coverage track was standardized to the same scale for each sample. Colors indicate size of siRNAs: black, 21 nt; red, 22 nt; blue, 24 nt.

The inverted duplications are of 3.2 Mb in *p1-ww-id1* and 0.3 Mb in *p1-ww-id4*; both Composite Insertions contain inverted repeats of the *Ac* 5′ terminal sequences, of 2.1–2.5 kb in *p1-ww-id1* and 1.8–3.9 kb in *p1-ww-id4*. These *Ac* inverted repeats are transcribed either from a flanking gene promoter in the case of *p1-ww-id1*, or possibly from the *Ac* promoter itself in the case of *p1-ww-id4*. dsRNA transcripts are detected from both alleles, presumably due to fold back pairing of the inverted repeat transcripts.

The alternative transposition-initiated *de novo* and heritable silencing in the *p1-ww-id* alleles is consistent with mechanisms of transcriptional gene silencing and post-transcriptional gene silencing reported for class 1 elements in *Arabidopsis* (*de novo* silencing: Marí-Ordóñez *et al.* 2013; Nuthikattu *et al.* 2013; McCue *et al.* 2014; Duan *et al.* 2015; Panda *et al.* 2016; heritable silencing: Law and Jacobsen 2010; Haag and Pikaard 2011; Castel and Martienssen 2013; Matzke and Mosher 2014). In the *p1-ww-id* alleles

described here, the 21- to 22-nt siRNAs enriched in the transcribed region of the Composite Insertions, and particularly in the loop region of *p1-ww-id4*, suggests the involvement of RDR6 in the *de novo* silencing. The reduced levels of *Ac* transcript can be formally explained by mRNA degradation via post-transcriptional gene silencing, and/or transcriptional gene silencing of the *Ac* promoter triggered by the Pol II-RDR6 pathway. Transcriptional silencing of *Ac* seems most likely, as silencing is maintained even after the *id1* and *id4* alleles are removed by meiotic segregation (Figure 3, B and C). The production of 24-nt siRNAs corresponding to the TIR and subterminal regions of *Ac* signals the possible involvement of the Pol IV-RDR2 RdDM pathway in the maintenance of transcriptional gene silencing by cytosine methylation in all sequence contexts (Law and Jacobsen 2010; Zemach *et al.* 2013; Stroud *et al.* 2014; Li *et al.* 2015b). The siRNA-independent pathway may also participate in the maintenance of symmetrical methylation (Stroud *et al.* 2013; Matzke and Mosher 2014).

The structure and effects of the *p1-ww-id1* and *p1-ww-id4* Composite Insertions are remarkably similar to the *Muk* allele that represses *Mutator* transposons in maize (Slotkin *et al.* 2003, 2005; Li *et al.* 2010; Burgess *et al.* 2020), and hence the *p1-ww-id1* and *p1-ww-id4* alleles can be considered as examples of "*killers*" targeting a different DNA TE superfamily. *Muk* and the *"Ac killers*" share similar features: (1) they are both initiated from naturally occurring inverted duplications of partial DNA transposon sequences; (2) the transcription of inverted duplications in *Muk* and *Ac killer* in *p1-ww-id1* are both driven by nearby promoters, while *p1-ww-id4* is possibly transcribed by the *Ac* promoter, producing dsRNAs as the precursor of 21-, 22-, and 24-nt siRNAs; and (3) both *Muk* and *Ac killer* can trigger in *trans* and heritable silencing of an active element. These similarities suggest a general mechanism for the heritable silencing of active DNA transposons [see Burgess *et al.* (2020)]. Active TEs are prone to rearrangements, some of which will be competent to silence otherwise active elements in *trans*. Thus, it is likely that if an element is active for sufficient time, it will eventually produce transposon killers. To the extent that selection favors a loss of TE activity, these killers would tend to spread within a population, eventually resulting in the heritable epigenetic silencing of homologous elements in that population. In addition to silencing resident active TEs, these killers may also serve as a reservoir of "antigens" that immunize genomes from subsequent invasion by active elements. Further, if expressed in specific cells of the male and female gametophyte, TE killers may serve as sources of small RNAs that reinforce TE silencing in germinal lineages (Martínez and Slotkin 2012).

Our discovery of siRNA-mediated *de novo* and heritable silencing of *Ac/Ds* adds another layer of complexity to the regulation of *Ac/Ds* activity. Previous studies of the regulation of *Ac/Ds* transposons reveal a complex relationship among *Ac* dosage, transcript abundance, transposase level, DNA methylation, and transposition frequency. *Ac* has a GC-rich subterminal region, and hypermethylation of this region is associated with transcriptional silencing (Kunze *et al.* 1988; Brutnell and Dellaporta 1994; Conrad and Brutnell 2005). It is this region of the *p1-ww-id* alleles that we see being targeted by 24-nt small RNAs. Given that these small RNAs are also observed in B73, they likely arise from inactive *Ac* elements present in that genetic background. Additionally, splicing of *Ac* mRNA is inefficient and inaccurate, producing a large number of aberrant *Ac* transcripts in *Arabidopsis*, representing post-transcriptional regulation (Jarvis *et al.* 1997). The aggregation of *Ac* transposase protein in tobacco (Kunze *et al.* 1995), petunia, and maize (Heinlein *et al.* 1994), may represent a type of post-translational regulation responsible for the *Ac* negative dosage effect first observed by McClintock (1948, 1949, 1950). Molecular analysis showed that increased dosage of *Ac* results in increased *Ac* transposase mRNA and protein levels, at least in the maize *wx-m7* allele that was tested (Fußwinkel *et al.* 1991). In this study, we find that the *p1-ww-id1* and *p1-ww-id4* alleles derived from alternative transposition-induced DNA rereplication initiate transgenerational silencing of active elements via *trans*-acting siRNAs.

These results also expand our understanding of the effect of alternative transposition on the structure of the maize genome. Previous studies have described the ability of alternative transposition to induce structural rearrangements such as deletions, inversions, translocations, duplications (Zhang and Peterson 2004; Huang and Dooner 2008; Zhang *et al.* 2009, 2013), and exon shuffling (Zhang *et al.* 2006; Wang *et al.* 2015). Here we show that *p1-ww-id* alleles derived from sister chromatid transposition contain novel inverted-repeat structures (Composite Insertions) generated by DNA rereplication. The fact that similar structures and mechanisms effect silencing in members of two unrelated transposon superfamilies (*hAT* and *Mu*) suggests that inverted repeat-induced siRNA may represent a general mechanism of spontaneous TE silencing.

Acknowledgments

We thank Dr. R. Keith Slotkin for suggestions on the dsRNA detection experiment, Lisa Coffey and Dr. Patrick Schnable for providing the growth chamber, Terry Olson for technical assistance, and Douglas Baker for field assistance. This research is supported by National Science Foundation award 0923826 (to T.P. and J.Z.), US Department of Agriculture National Institute of Food and Agriculture Hatch project number IOW05282, State of Iowa funds, and an Institutional Development Award from the National Institute of General Medical Sciences of the National Institutes of Health (grant P20-GM103476).

Author contributions: D.W., J.Z., and T.P. conceived and designed the experiment; D.W. performed the experiments; T.Z., M.Z., and D.W. analyzed the small RNA-sequencing data; D.W., D.L., and T.P. wrote the paper.

Note added in proof: See Burgess *et al.* 2020 (pp. 379–391) in this issue for a related work.

Literature Cited

Allen, G. C., M. A. Flores-Vergara, S. Krasynanski, S. Kumar, and W. F. Thompson, 2006 A modified protocol for rapid DNA isolation from plant tissues using cetyltrimethylammonium bromide. Nat. Protoc. 1: 2320–2325. https://doi.org/10.1038/nprot.2006.384

Anderson, S. N., M. C. Stitzer, P. Zhou, J. Ross-Ibarra, C. D. Hirsch *et al.*, 2019 Dynamic patterns of transcript abundance of transposable element families in maize. *G3 (Bethesda)* 9: 3673–3682.. https://doi.org/10.1534/g3.119.400431

Brink, R. A., and R. A. Nilan, 1952 The relation between light variegated and medium variegated pericarp in maize. Genetics 37: 519–544.

Brutnell, T. P., and S. L. Dellaporta, 1994 Somatic inactivation and reactivation of Ac associated with changes in cytosine methylation and transposase expression. Genetics 138: 213–225.

Burgess, D., H. Li, M. Zhao, S. Y. Kim, and D. Lisch, 2020 Silencing of Mu elements in maize involves distinct populations of small RNAs and distinct patterns of DNA methylation. Genetics Early online March 30, 2020. https://doi.org/10.1534/genetics.120.303033

Castel, S. E., and R. A. Martienssen, 2013 RNA interference in the nucleus: roles for small RNAs in transcription, epigenetics and beyond. Nat. Rev. Genet. 14: 100–112. https://doi.org/10.1038/nrg3355

Chen, J., I. M. Greenblatt, and S. L. Dellaporta, 1987 Transposition of Ac from the P locus of maize into unreplicated chromosomal sites. Genetics 117: 109–116.

Chitwood, D. H., and M. C. P. Timmermans, 2010 Small RNAs are on the move. Nature 467: 415–419. https://doi.org/10.1038/nature09351

Conrad, L. J., and T. P. Brutnell, 2005 Ac-Immobilized, a stable source of Activator transposase that mediates sporophytic and gametophytic excision of Dissociation elements in maize. Genetics 171: 1999–2012. https://doi.org/10.1534/genetics.105.046623

Döring, H. P., and P. Starlinger, 1984 Barbara McClintock's controlling elements: now at the DNA level. Cell 39: 253–259. https://doi.org/10.1016/0092-8674(84)90002-3

Duan, C.-G., H. Zhang, K. Tang, X. Zhu, W. Qian *et al.*, 2015 Specific but interdependent functions for Arabidopsis AGO4 and AGO6 in RNA-directed DNA methylation. EMBO J. 34: 581–592. https://doi.org/10.15252/embj.201489453

Dunoyer, P., G. Schott, C. Himber, D. Meyer, A. Takeda *et al.*, 2010 Small RNA duplexes function as mobile silencing signals between plant cells. Science 328: 912–916. https://doi.org/10.1126/science.1185880

Fußwinkel, H., S. Schein, U. Courage, P. Starlinger, and R. Kunze, 1991 Detection and abundance of mRNA and protein encoded by transposable element Activator (Ac) in maize. Mol. Gen. Genet. 225: 186–192. https://doi.org/10.1007/BF00269846

Gray, Y. H. M., 2000 It takes two transposons to tango: transposable-element-mediated chromosomal rearrangements. Trends Genet. 16: 461–468. https://doi.org/10.1016/S0168-9525(00)02104-1

Greenblatt, I., and R. Brink, 1962 Twin mutations in medium variegated pericarp maize. Genetics 47: 489–501.

Haag, J. R., and C. S. Pikaard, 2011 Multisubunit RNA polymerases IV and V: purveyors of non-coding RNA for plant gene silencing. Nat. Rev. Mol. Cell Biol. 12: 483–492. https://doi.org/10.1038/nrm3152

Heinlein, M., T. Brattig, and R. Kunze, 1994 In vivo aggregation of maize Activator (Ac) transposase in nuclei of maize endosperm and petunia protoplasts. Plant J. 5: 705–714. https://doi.org/10.1111/j.1365-313X.1994.00705.x

Huang, J. T., and H. K. Dooner, 2008 Macrotransposition and other complex chromosomal restructuring in maize by closely linked transposons in direct orientation. Plant Cell 20: 2019–2032. https://doi.org/10.1105/tpc.108.060582

Jarvis, P., F. Belzile, and C. Dean, 1997 Inefficient and incorrect processing of the Ac transposase transcript in iae1 and wild-type Arabidopsis thaliana. Plant J. 11: 921–931. https://doi.org/10.1046/j.1365-313X.1997.11050921.x

Kermicle J. L., 1980 Probing the component structure of a maize gene with transposable elements. Science 208: 1457–1459. https://doi.org/10.1126/science.208.4451.1457

Kidwell, M. G., 1985 Hybrid dysgenesis in Drosophila melanogaster: nature and inheritance of P element regulation. Genetics 111: 337–350.

Kunze, R., P. Starlinger, and D. Schwartz, 1988 DNA methylation of the maize transposable element Ac interferes with its transcription. Mol. Gen. Genet. 214: 325–327. https://doi.org/10.1007/BF00337730

Kunze, R., S. Kuhn, J. D. G. Jones, and S. R. Scofield, 1995 Somatic and germinal activities of maize Activator (Ac) transposase mutants in transgenic tobacco. Plant J. 8: 45–54. https://doi.org/10.1046/j.1365-313X.1995.08010045.x

Langmead, B., C. Trapnell, M. Pop, and S. L. Salzberg, 2009 Ultrafast and memory-efficient alignment of short DNA sequences to the human genome. Genome Biol. 10: R25. https://doi.org/10.1186/gb-2009-10-3-r25

Law, J. A., and S. E. Jacobsen, 2010 Establishing, maintaining and modifying DNA methylation patterns in plants and animals. Nat. Rev. Genet. 11: 204–220. https://doi.org/10.1038/nrg2719

Lechelt, C., T. Peterson, A. Laird, J. Chen, S. L. Dellaporta *et al.*, 1989 Isolation and molecular analysis of the maize P locus. Mol. Gen. Genet. 219: 225–234. https://doi.org/10.1007/BF00261181

Li, H., M. Freeling, and D. Lisch, 2010 Epigenetic reprogramming during vegetative phase change in maize. Proc. Natl. Acad. Sci. USA 107: 22184–22189. https://doi.org/10.1073/pnas.1016884108

Li, Q., J. I. Gent, G. Zynda, J. Song, I. Makarevitch *et al.*, 2015a RNA-directed DNA methylation enforces boundaries between heterochromatin and euchromatin in the maize genome. Proc. Natl. Acad. Sci. USA 112: 14728–14733. https://doi.org/10.1073/pnas.1514680112

Li, S., L. E. Vandivier, B. Tu, L. Gao, and S. Y. Won, 2015b Detection of Pol IV/RDR2-dependent transcripts at the genomic scale in Arabidopsis reveals features and regulation of siRNA biogenesis. Genome Res. 25: 235–245. https://doi.org/10.1101/gr.182238.114

Lisch, D., 2002 Mutator transposons. Trends Plant Sci. 7: 498–504. https://www.ncbi.nlm.nih.gov/pubmed/12417150

Marí-Ordóñez, A., A. Marchais, M. Etcheverry, A. Martin, V. Colot *et al.*, 2013 Reconstructing de novo silencing of an active plant retrotransposon. Nat. Genet. 45: 1029–1039. https://doi.org/10.1038/ng.2703

Martínez, G., and R. K. Slotkin, 2012 Developmental relaxation of transposable element silencing in plants: functional or byproduct? Curr. Opin. Plant Biol. 15: 496–502. https://doi.org/10.1016/j.pbi.2012.09.001

Matsumoto, T., J. Wu, H. Kanamori, Y. Katayose, M. Fujisawa *et al.*, 2005 The map-based sequence of the rice genome. Nature 436: 793–800. https://doi.org/10.1038/nature03895

Matzke, M. A., and R. A. Mosher, 2014 RNA-directed DNA methylation: an epigenetic pathway of increasing complexity. Nat. Rev. Genet. 15: 394–408 (erratum: Nat. Rev. Genet. 15: 570). https://doi.org/10.1038/nrg3683

Matzke, M. A., T. Kanno, and A. J. M. Matzke, 2015 RNA-directed DNA methylation: the evolution of a complex epigenetic pathway in flowering plants. Annu. Rev. Plant Biol. 66: 243–267. https://doi.org/10.1146/annurev-arplant-043014-114633

McClintock, B., 1948 Mutable loci in maize. Carnegie Inst. Washingt. Year B. 47: 155–169.

McClintock, B., 1949 Mutable loci in maize: the mechanism of transposition of the Ds Locus. Carnegie Inst. Washingt. Year B. 48: 142–154.

McClintock, B., 1950 Mutable loci in maize: mode of detection of transpositions of Ds. Carnegie Inst. Washingt. Year B 49: 157–167.
McClintock, B., 1951 Chromosome organization and genic expression. Cold Spring Harb. Symp. Quant. Biol. 16: 13–47. https://doi.org/10.1101/SQB.1951.016.01.004
McCue, A. D., K. Panda, S. Nuthikattu, S. G. Choudury, E. N. Thomas *et al.*, 2014 ARGONAUTE 6 bridges transposable element mRNA-derived siRNAs to the establishment of DNA methylation. EMBO J. 34: 20–35. https://doi.org/10.15252/embj.201489499
Molnar, A., C. W. Melnyk, A. Bassett, T. J. Hardcastle, R. Dunn *et al.*, 2010 Small silencing RNAs in plants are mobile and direct epigenetic modification in recipient cells. Science 328: 872–875. https://doi.org/10.1126/science.1187959
Nuthikattu, S., A. D. McCue, K. Panda, D. Fultz, C. DeFraia *et al.*, 2013 The initiation of epigenetic silencing of active transposable elements is triggered by RDR6 and 21–22 nucleotide small interfering RNAs. Plant Physiol. 162: 116–131. https://doi.org/10.1104/pp.113.216481
Panda, K., L. Ji, D. A. Neumann, J. Daron, R. J. Schmitz *et al.*, 2016 Full-length autonomous transposable elements are preferentially targeted by expression-dependent forms of RNA-directed DNA methylation. Genome Biol. 17: 170. https://doi.org/10.1186/s13059-016-1032-y
Paterson, A. H., J. E. Bowers, R. Bruggmann, I. Dubchak, J. Grimwood *et al.*, 2009 The Sorghum bicolor genome and the diversification of grasses. Nature 457: 551–556. https://doi.org/10.1038/nature07723
Peacock, W. J., E. S. Dennis, W. L. Gerlach, M. M. Sachs, and D. Schwartz, 1984 Insertion and excision of Ds controlling elements in maize. Cold Spring Harb. Symp. Quant. Biol. 49: 347–354. https://doi.org/10.1101/SQB.1984.049.01.041
Pikaard, C. S., 2013 Methylating the DNA of the most repressed: special access required. Mol. Cell 49: 1021–1022. https://doi.org/10.1016/j.molcel.2013.03.013
Pohlman, R. F., N. V. Fedoroff, and J. Messing, 1984 The nucleotide sequence of the maize controlling element Activator. Cell 37: 635–643. https://doi.org/10.1016/0092-8674(84)90395-7
Pontier, D., C. Picart, F. Roudier, D. Garcia, S. Lahmy *et al.*, 2012 NERD, a plant-specific GW protein, defines an additional RNAi-dependent chromatin-based pathway in Arabidopsis. Mol. Cell 48: 121–132. https://doi.org/10.1016/j.molcel.2012.07.027
Regulski, M., Z. Lu, J. Kendall, M. T. Donoghue, J. Reinders *et al.*, 2013 The maize methylome influences mRNA splice sites and reveals widespread paramutation-like switches guided by small RNA. Genome Res. 23: 1651–1662. https://doi.org/10.1101/gr.153510.112
Robinson, J. T., H. Thorvaldsdóttir, W. Winckler, M. Guttman, E. S. Lander *et al.*, 2011 Integrative genomics viewer. Nat. Biotechnol. 29: 24–26. https://doi.org/10.1038/nbt.1754
Ros, F., and R. Kunze, 2001 Regulation of Activator/Dissociation transposition by replication and DNA methylation. Genetics 157: 1723–1733.
Sambrook, J.,F. E. Fritsch., and T. Maniatis, 1989 *Molecular Cloning: A Laboratory Manual*, 2nd ed., Cold Spring Harbor Laboratory, Cold Spring Harbor, N.Y.
Sanmiguel, P., and C. Vitte, 2009 The LTR-retrotransposons of maize, pp. 307–327 in *Maize Handbook - Volume II: Genetics and Genomics*, edited by J. L. Bennetzen, S. C. Hake Springer-Verlag, New York.
Schnable P. S., D. Ware, R. S. Fulton, J. C. Stein, F. Wei, *et al.*, 2009 The B73 maize genome: complexity, diversity, and dynamics. Science 326: 1112–1115. https://doi.org/10.1126/science.1178534
Slotkin, R. K., M. Freeling, and D. Lisch, 2003 Mu killer causes the heritable inactivation of the Mutator family of transposable elements in Zea mays. Genetics 165: 781–797.
Slotkin, R. K., M. Freeling, and D. Lisch, 2005 Heritable transposon silencing initiated by a naturally occurring transposon inverted duplication. Nat. Genet. 37: 641–644. https://doi.org/10.1038/ng1576
Stroud, H., M. V. C. Greenberg, S. Feng, Y. V. Bernatavichute, and S. E. Jacobsen, 2013 Comprehensive analysis of silencing mutants reveals complex regulation of the Arabidopsis methylome. Cell 152: 352–364 [corrigenda: Cell 161: 1697–1698 (2015)]. https://doi.org/10.1016/j.cell.2012.10.054
Stroud, H., T. Do, J. Du, X. Zhong, S. Feng *et al.*, 2014 Non-CG methylation patterns shape the epigenetic landscape in Arabidopsis. Nat. Struct. Mol. Biol. 21: 64–72. https://doi.org/10.1038/nsmb.2735
Tikhonov, A. P., P. J. SanMiguel, Y. Nakajima, N. M. Gorenstein, J. L. Bennetzen *et al.*, 1999 Colinearity and its exceptions in orthologous adh regions of maize and sorghum. Proc. Natl. Acad. Sci. USA 96: 7409–7414. https://doi.org/10.1073/pnas.96.13.7409
Vollbrecht, E., J. Duvick, J. P. Schares, K. R. Ahern, P. Deewatthanawong *et al.*, 2010 Genome-wide distribution of transposed dissociation elements in maize. Plant Cell 22: 1667–1685. https://doi.org/10.1105/tpc.109.073452
Wang, X., A. A. Elling, X. Li, N. Li, Z. Peng *et al.*, 2009 Genome-wide and organ-specific landscapes of epigenetic modifications and their relationships to mRNA and small RNA transcriptomes in maize. Plant Cell 21: 1053–1069. https://doi.org/10.1105/tpc.109.065714
Wang, D., C. Yu, T. Zuo, J. Zhang, D. F. Weber *et al.*, 2015 Alternative transposition generates new chimeric genes and segmental duplications at the maize p1 locus. Genetics 201: 925–935. https://doi.org/10.1534/genetics.115.178210
Weil, C. F., and S. R. Wessler, 1993 Molecular evidence that chromosome breakage by Ds elements is caused by aberrant transposition. Plant Cell 5: 515–522. https://doi.org/10.1105/tpc.5.5.515
West, P. T., Q. Li, L. Ji, S. R. Eichten, J. Song *et al.*, 2014 Genomic distribution of H3K9me2 and DNA methylation in a maize genome. PLoS One 9: e105267. https://doi.org/10.1371/journal.pone.0105267
Zemach, A., M. Y. Kim, P. H. Hsieh, D. Coleman-Derr, L. Eshed-Williams *et al.*, 2013 The arabidopsis nucleosome remodeler DDM1 allows DNA methyltransferases to access H1-containing heterochromatin. Cell 153: 193–205. https://doi.org/10.1016/j.cell.2013.02.033
Zhang, J., and T. Peterson, 1999 Genome rearrangements by nonlinear transposons in maize. Genetics 153: 1403–1410.
Zhang, J., and T. Peterson, 2004 Transposition of reversed Ac element ends generates chromosome rearrangements in maize. Genetics 167: 1929–1937. https://doi.org/10.1534/genetics.103.026229
Zhang, J., F. Zhang, and T. Peterson, 2006 Transposition of reversed Ac element ends generates novel chimeric genes in maize. PLoS Genet. 2: e164. https://doi.org/10.1371/journal.pgen.0020164
Zhang, J., C. Yu, V. Pulletikurti, J. Lamb, T. Danilova *et al.*, 2009 Alternative Ac/Ds transposition induces major chromosomal rearrangements in maize. Genes Dev. 23: 755–765. https://doi.org/10.1101/gad.1776909
Zhang, J., T. Zuo, and T. Peterson, 2013 Generation of tandem direct duplications by reversed-ends transposition of maize Ac elements. PLoS Genet. 9: e1003691. https://doi.org/10.1371/journal.pgen.1003691
Zhang, J., T. Zuo, D. Wang, and T. Peterson, 2014 Transposition-mediated DNA re-replication in maize. eLife 3: e03724. https://doi.org/10.7554/eLife.03724
Zuo, T., J. Zhang, A. Lithio, S. Dash, D. F. Weber *et al.*, 2016 Genes and small RNA transcripts exhibit dosage-dependent expression pattern in maize copy-number alterations. Genetics 203: 1133–1147. https://doi.org/10.1534/genetics.116.188235

Communicating editor: J. Birchler